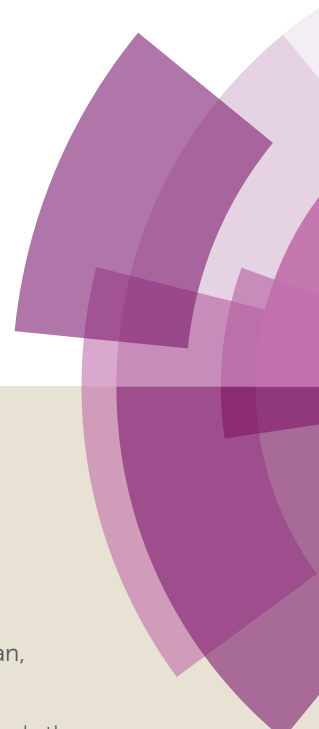
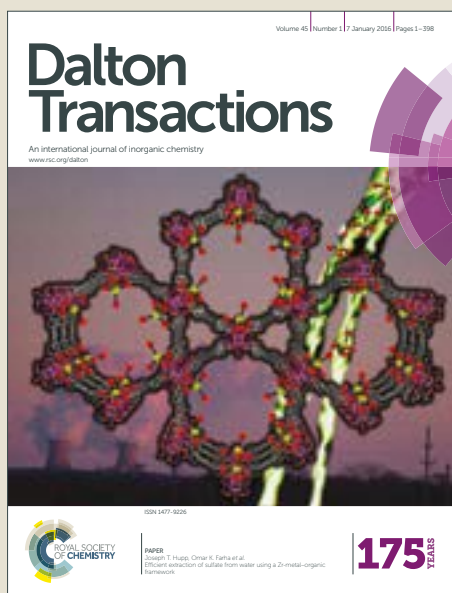


Dalton Transactions

Accepted Manuscript



This article can be cited before page numbers have been issued, to do this please use: T. Zheng, L. Qian, M. Li, Z. Wang, K. Li, Y. Zhang, B. Li and B. Wu, *Dalton Trans.*, 2018, DOI: 10.1039/C8DT01685B.



This is an Accepted Manuscript, which has been through the Royal Society of Chemistry peer review process and has been accepted for publication.

Accepted Manuscripts are published online shortly after acceptance, before technical editing, formatting and proof reading. Using this free service, authors can make their results available to the community, in citable form, before we publish the edited article. We will replace this Accepted Manuscript with the edited and formatted Advance Article as soon as it is available.

You can find more information about Accepted Manuscripts in the [author guidelines](#).

Please note that technical editing may introduce minor changes to the text and/or graphics, which may alter content. The journal's standard [Terms & Conditions](#) and the ethical guidelines, outlined in our [author and reviewer resource centre](#), still apply. In no event shall the Royal Society of Chemistry be held responsible for any errors or omissions in this Accepted Manuscript or any consequences arising from the use of any information it contains.



Journal Name

ARTICLE

A bifunctional cationic metal-organic framework based on unprecedented nonanuclear copper(II) cluster for high dichromate and chromate trapping and highly efficient photocatalytic degradation of organic dyes under visible light irradiation†

Received 00th January 20xx,
Accepted 00th January 20xx

DOI: 10.1039/x0xx00000x

www.rsc.org/

Tian-Rui Zheng, Lin-Lu Qian, Min Li, Zhi-Xiang Wang, Ke Li, Ya-Qian Zhang, Bao-Long Li* and Bing Wu

A bifunctional cationic metal-organic framework $\{[\text{Cu}_9(\text{OH})_6\text{Cl}_2(\text{itp})_6(1,4\text{-bdc})_3](\text{NO}_3)_2(\text{OH})_2 \cdot 20\text{H}_2\text{O}\}_n$ (**1-NO₃-OH-20H₂O**) was synthesized and characterized (itp = 1-imidazol-1-yl-3-(1,2,4-triazol-4-yl)propane, 1,4-bdc = 1,4-benzenedicarboxylate). In **1-NO₃-OH-20H₂O**, three $[\text{Cu}_3(\mu_3\text{-OH})(\mu_2\text{-OH})]$ trimeric clusters are bridged by two $\mu_3\text{-Cl}$ and form $[\text{Cu}_9(\mu_3\text{-OH})_3(\mu_2\text{-OH})_3(\mu_3\text{-Cl})_2]$ cluster. Such nonanuclear copper(II) cluster $[\text{Cu}_9(\mu_3\text{-OH})_3(\mu_2\text{-OH})_3(\mu_3\text{-Cl})_2]$ is not reported until now, as to our best knowledge. **1-NO₃-OH-20H₂O** shows a 6-connected 2D 3^6-hxl net based on nonanuclear copper(II) cluster $[\text{Cu}_9(\mu_3\text{-OH})_3(\mu_2\text{-OH})_3(\mu_3\text{-Cl})_2]$. **1-NO₃-OH-20H₂O** is also the first 2D 3^6-hxl net based nonanuclear cluster. **1-NO₃-OH** (guest-free phase) shows fast and high efficient $\text{Cr}_2\text{O}_7^{2-}$ and CrO_4^{2-} trapping, and good recyclability for capturing of $\text{Cr}_2\text{O}_7^{2-}$ and CrO_4^{2-} . The adsorption capacities of **1-NO₃-OH** to capture $\text{Cr}_2\text{O}_7^{2-}$ and CrO_4^{2-} are $1.762 \text{ mol mol}^{-1}$ (154.8 mg g^{-1}) and $1.896 \text{ mol mol}^{-1}$ (89.5 mg g^{-1}), respectively at molar ratio 1:2 (**1-NO₃-OH** to $2.5 \times 10^{-3} \text{ mol/L}$ $\text{Cr}_2\text{O}_7^{2-}$ or CrO_4^{2-}). **1-NO₃-OH** exhibits selective sorption of $\text{Cr}_2\text{O}_7^{2-}$ or CrO_4^{2-} from the solution containing mixture of $\text{Cr}_2\text{O}_7^{2-}$ or CrO_4^{2-} and tenfold the molar amount of ClO_4^- , NO_3^- , Cl^- , BF_4^- or fivefold the molar amount of mol/L SO_4^{2-} . **1-NO₃-OH** can capture 87.9% dilute $\text{Cr}_2\text{O}_7^{2-}$ or 91.8% dilute CrO_4^{2-} at equimolar **1-NO₃-OH** to 20 ppm $\text{Cr}_2\text{O}_7^{2-}$ or CrO_4^{2-} . **1-NO₃-OH-20H₂O** exhibits highly efficient photocatalytic degradation of the cationic organic dyes methylene blue (MB) and rhodamine B (RhB) under visible light irradiation, and is a good photocatalyst for photocatalytic degradation of the cationic organic dyes.

Introduction

Water pollution has been becoming a serious global environmental pollution issue with the development of modern industry and living.¹ Hexavalent chromium Cr(VI) was classified as Group "A" human carcinogen by U.S. Environment Protection Agency (EPA) because it causes serious damages to human health.^{2,3} The elimination of $\text{Cr}_2\text{O}_7^{2-}$ and CrO_4^{2-} from wastewater is very urgently desirable. But conventional technologies such as adsorbents, resin and membranes are poor selectivity, low adsorption capacities and slow process kinetics.⁴ Therefore, the research and development of advanced technologies and new materials for $\text{Cr}_2\text{O}_7^{2-}$ and CrO_4^{2-} treatment is quite essential.

Organic dyes which are widely used in dyeing, dyestuffs and the textile industry, are main contamination of wastewater due to their poor biodegradability.⁵ Currently, semiconductor compounds such as metal oxides TiO_2 , ZnO, CdO, metal sulfides ZnS, CdS and their composites are usually employed as photocatalysts for

photocatalytic degradation of organic dyes.⁶ TiO_2 , ZnO and CdO are likely the most important semiconductors for photocatalysis. But the relative high band gaps (E_g) of TiO_2 (3.2 eV), ZnO (3.4 eV) and CdO (2.5 eV) make them absorbing mere a small amount of ultraviolet light from visible or sunlight and therefore, limit their fast development and wide applications.⁷ The research and development of the high efficient photocatalysts under visible light or sunlight irradiation is greatly valuable.

Metal-organic frameworks (MOFs) have attracted great attention because of their diverse topologies and widely potential applications as functional materials in catalysis, gas adsorption, magnetism, chemical sensors, separation and so on.^{8,9} Cationic MOFs contain substitutable uncoordinated anions in their cavity, and therefore, could serve as the anion-exchange hosts for capture anions and contaminant removal.¹⁰ Until to now, only few cationic MOFs have been reported for the removal of $\text{Cr}_2\text{O}_7^{2-}$ or CrO_4^{2-} from aqueous media.¹¹⁻¹⁴ For example, Olive and co-workers synthesized a 2D cationic Ag-MOF (**SLUG-21**) as an adsorbent of CrO_4^{2-} through anion exchange.^{11a} Ghost and co-workers reported a water-stable cationic MOF (**1'SO₄²⁻**) as an adsorbent of $\text{Cr}_2\text{O}_7^{2-}$ through anion exchange.^{12b} Our group synthesized a cationic MOF $\{[\text{Cu}_4(\mu_3\text{-OH})_2(\text{mtrb})_2(1,4\text{-bda})_2]\text{Br}_2 \cdot 6\text{H}_2\text{O}\}_n$ (**1-Br**) which shows fast and highly efficient $\text{Cr}_2\text{O}_7^{2-}$ trapping through the SC-SC process.^{13c} Scarce cationic MOFs were reported as adsorbents for removal both $\text{Cr}_2\text{O}_7^{2-}$ and CrO_4^{2-} . For example, Lazarides and co-workers reported a Zr cationic MOF (**MOR-2**) structural characterized via power X-

State and Local Joint Engineering Laboratory for Functional Polymeric Materials, College of Chemistry, Chemical Engineering and Materials Science, Soochow University, Suzhou 215123, PR China. E-mail: libaolong@suda.edu.cn

†Electronic Supplementary Information (ESI) available: Table and additional Figures. CCDC 1832270. For ESI and crystallographic data in CIF or other electronic format see DOI: 10.1039/x0xx00000x

ray crystallography and its composite form (**MOR-2-HA**) as adsorbents of removal both $\text{Cr}_2\text{O}_7^{2-}$ and CrO_4^{2-} .¹⁴

Garcia and co-workers reported MOF-5 as the first MOF semiconductor photocatalyst for the degradation of phenol.¹⁵ Although, some MOF photocatalysts for the degradation of organic dyes under UV or visible light irradiation were reported.¹⁶⁻¹⁸ However, relative few MOFs exhibit effective photocatalytic activity under visible light irradiation due to most of MOFs with poor photoresponse in the visible region.^{17,18} In previous work, we synthesized some Cu-MOFs using flexible N-donor ligands and multicarboxylate ligands which show good photocatalytic activity in the degradation of organic dyes under UV or visible light irradiation.¹⁹

In the present work, a bifunctional Cu-MOF $\{[\text{Cu}_9(\text{OH})_6\text{Cl}_2(\text{itp})_6(1,4\text{-bdc})_3](\text{NO}_3)_2(\text{OH})_2 \cdot 20\text{H}_2\text{O}\}_n$ (**1-NO₃-OH·20H₂O**) (itp = 1-imidazol-1-yl-3-(1,2,4-triazol-4-yl)propane, 1,4-bdc = 1,4-benzenedicarboxylate) was synthesized by the hydrothermal method. **1-NO₃-OH·20H₂O** shows a 6-connected 2D 3⁶-hxl net based on unprecedented nonanuclear copper(II) cluster $[\text{Cu}_9(\mu_3\text{-OH})_3(\mu_2\text{-OH})_3(\mu_3\text{-Cl})_2]$. **1-NO₃-OH** (guest-free phase) shows fast and high efficient $\text{Cr}_2\text{O}_7^{2-}$ and CrO_4^{2-} trapping, and good recyclability for capturing of $\text{Cr}_2\text{O}_7^{2-}$ and CrO_4^{2-} . **1-NO₃-OH·20H₂O** exhibits highly efficient photocatalytic degradation of the cationic organic dyes methylene blue (MB) and rhodamine B (RhB) under visible light irradiation.

Experimental

Materials and methods.

All reagents were purchased and used without further purification. Elemental analyses for C, H and N were performed on a Perkin-Elmer 240C analyzer. FT-IR spectra were obtained on a Bruker VERTEX 70 FT-IR spectrophotometer in the 4000–600 cm^{-1} region. Powder X-ray diffraction (PXRD) were performed on a D/MAX-3C diffractometer with the Cu-K α radiation ($\lambda = 1.5406 \text{ \AA}$) at room temperature. The UV-vis spectra were measured on a Varian Cary 500 UV-vis spectrophotometer. UV-vis diffuse reflectance spectra of the solid samples were collected using a Cary 500 spectrophotometer using barium sulfate (BaSO_4) as a reflectance standard. The X-ray photoelectron spectra (XPS) were recorded on an ESCALAB250XI spectrometer (Thermo-VG Scientific) and the binding energy values were calibrated with respect to the C (1s) peak (284.6 eV).

Synthesis of $\{[\text{Cu}_9(\text{OH})_6\text{Cl}_2(\text{itp})_6(1,4\text{-bdc})_3](\text{NO}_3)_2(\text{OH})_2 \cdot 20\text{H}_2\text{O}\}_n$ (**1-NO₃-OH·20H₂O**)

A mixture of itp (0.035 g, 0.2 mmol), 1,4-H₂bdc (0.017 g, 0.1 mmol), $\text{Cu}(\text{NO}_3)_2 \cdot 3\text{H}_2\text{O}$ (0.048 g, 0.2 mmol), $\text{CuCl}_2 \cdot 2\text{H}_2\text{O}$ (0.034 g, 0.2 mmol), NaOH (0.008 g, 0.20 mmol) and H₂O (6.5 mL) were added to a Teflon-lined stainless autoclave and this was sealed and heated to 90°C for 2 days and then cooled to room temperature. The blue crystals **1-NO₃-OH·20H₂O** were obtained in 31% yield based on itp (0.029 g). Anal. Calc. for $\text{C}_{78}\text{H}_{126}\text{Cl}_2\text{Cu}_9\text{N}_3\text{O}_{46}$ (**1-NO₃-OH·20H₂O**): C, 33.24%; H, 4.51%; N, 15.90%. Found: C, 33.15%; H, 4.45%; N, 15.78%. IR data (cm^{-1}): 3402m, 3123w, 1636w, 1570s, 1452w, 1373s, 1288w, 1259w, 1229w, 1200w, 1099m, 964w, 885w, 864w, 825w, 758m, 663w, 629m. These blue crystals **1-NO₃-OH·20H₂O**

were heated under vacuum at 75°C for one day to obtain the quest free phase dark teal crystals **1-NO₃-OH**.

X-ray Crystallography

The measurement of **1-NO₃-OH·20H₂O** was made by using a Rigaku Saturn CCD diffractometer with an enhanced X-ray source Mo K α ($\lambda = 0.71073 \text{ \AA}$). The single crystal was mounted on a glass fiber at 293 K. The structure was solved and refined with SHELXTL package.²⁰ The disordered hydroxy anions and water molecules in **1-NO₃-OH·20H₂O** were removed with the SQUEEZE procedure in PLATON. The positions of the hydrogen atoms of itp and 1,4-bdc ligands were determined with theoretical calculations. The parameters of the crystal data collection and refinement of **1-NO₃-OH·20H₂O** are given in Table S1 (in the ESI[†]). Selected bond lengths and angles are listed in Table S2 (in the ESI[†]).

Anion Exchange Studies

General procedure

Molar ratio 1:1 (**1-NO₃-OH** to 20 ppm $\text{Cr}_2\text{O}_7^{2-}$ or CrO_4^{2-}), Selective capture of $\text{Cr}_2\text{O}_7^{2-}$, Selective capture of CrO_4^{2-} , Release and cycle experiment are shown in the ESI[†].

(a) Molar ratio 1:2 (**1-NO₃-OH** to $2.5 \times 10^{-3} \text{ mol/L Cr}_2\text{O}_7^{2-}$ or CrO_4^{2-})

$\{[\text{Cu}_9(\text{OH})_6\text{Cl}_2(\text{itp})_6(1,4\text{-bdc})_3](\text{NO}_3)_2(\text{OH})_2\}_n$ (**1-NO₃-OH**) (20 mg, 0.00814 mmol) was immersed in a 6.5 mL $2.5 \times 10^{-3} \text{ mol/L Cr}_2\text{O}_7^{2-}$ or CrO_4^{2-} aqueous solution and the mixture was mildly shaken at room temperature. The anion exchange process was monitored by liquid UV-vis spectroscopy based on typical absorption of $\text{Cr}_2\text{O}_7^{2-}$ at 257 nm or CrO_4^{2-} at 372 nm. 0.10 mL $\text{Cr}_2\text{O}_7^{2-}$ or CrO_4^{2-} aqueous solution was pipetted at different time interval and was diluted using 1.9 mL deionized water to measure the UV-vis adsorption intensity.

The equilibrium adsorption capacity q_e (mg/g) is calculated by the following equation.

$$q_e = \frac{(C_i - C_e)V}{W} \quad (1)$$

Where C_i and C_e (mg/L) were the initial and final concentrations of $\text{Cr}_2\text{O}_7^{2-}$, respectively. V (L) was the volume of the solution, and W (g) was the mass of sorbent.

(b) Molar ratio 1:1 (**1-NO₃-OH** to $2.5 \times 10^{-3} \text{ mol/L Cr}_2\text{O}_7^{2-}$ or CrO_4^{2-})

The procedure is similar to that of the experiment of molar ratio 1:2, except that **1-NO₃-OH** (40 mg, 0.0163 mmol) was used in this experiment.

Photocatalytic experiment

The experiment was carried out a PCR-I multipurpose photoreactor (Beijing China Education Au-Light Company Limited, China) equipped a CEL-HXF300 Xe lamp with UV cut-off filter (providing visible light with $\lambda > 400 \text{ nm}$). **1-NO₃-OH·20H₂O** (40 mg) and 0.50 mL 30% H₂O₂ were added into a 100 mL of methylene blue (MB) solution (10 mg/L), or a 100 mL of rhodamine B (RhB) solution (10 mg/L). The suspension solution was stirred in the dark for about 30 min. Then, the mixture was stirred continuously under visible light irradiation. At a given interval, aliquots of the reaction mixture were periodically taken and analyzed with a UV-vis spectrophotometer at

an absorption wavelength of 664 nm for MB and 552 nm for RhB. The blank experiment in the presence of H₂O₂ and absence of

photocatalyst **1-NO₃-OH-20H₂O** was also measured.

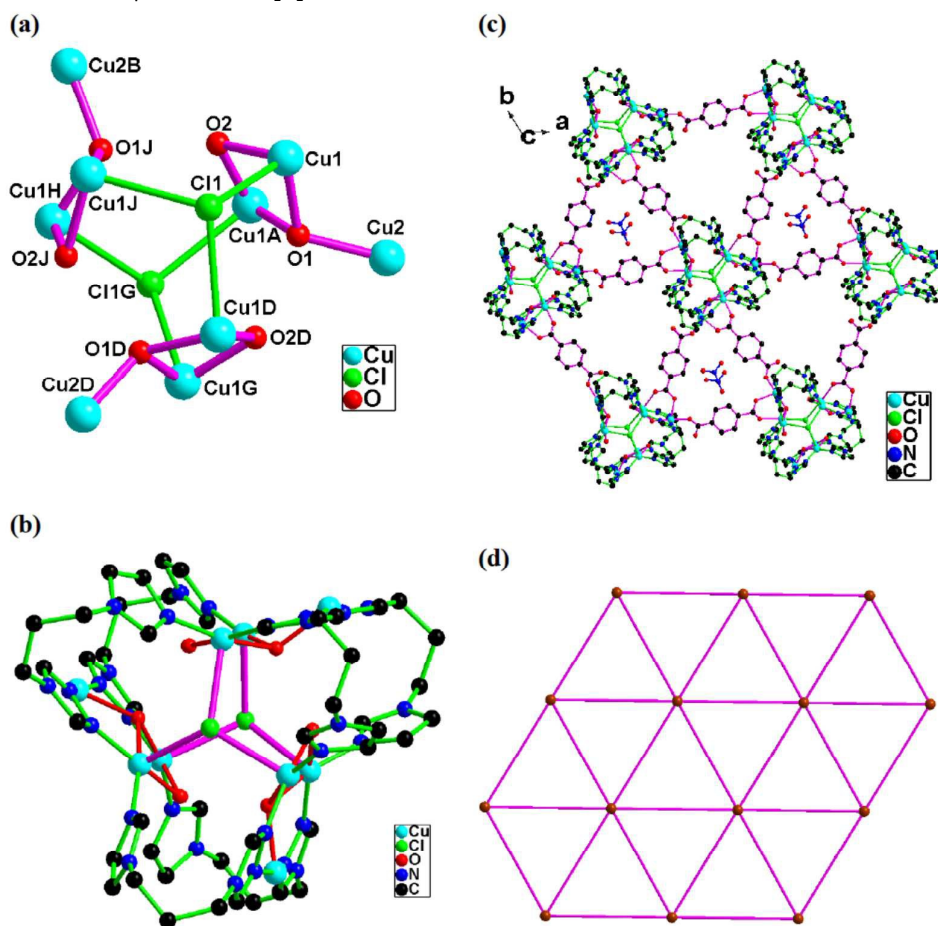


Fig. 1 (a) The [Cu₉(OH)₆Cl₂] nonanuclear copper(II) cluster in **1-NO₃-OH-20H₂O**; (b) The [Cu₉(OH)₆Cl₂(itp)₆] nonanuclear copper(II) cluster in **1-NO₃-OH-20H₂O**; (c) The 2D cationic network in **1-NO₃-OH-20H₂O**, showing nitrate anions in the cavity; (d) Schematic depiction of the 6-connected 2D network in **1-NO₃-OH-20H₂O**. The brown balls show the 6-connected [Cu₉(OH)₆Cl₂(itp)₆] clusters. The pink sticks exhibit the 2-connected 1,4-bdc ligands.

Results and Discussion

Crystal structure of $\{[Cu_9(OH)_6Cl_2(itp)_6(1,4-bdc)_3](NO_3)_2(OH)_2 \cdot 20H_2O\}_n$ (**1-NO₃-OH-20H₂O**)

1-NO₃-OH-20H₂O shows a 6-connected 2D 3⁶-hxl net based on unprecedented nonanuclear copper(II) cluster [Cu₉(μ₃-OH)₃(μ₂-OH)₃(μ₃-Cl)₂]. The asymmetric unit of **1-NO₃-OH-20H₂O** consists of one and half Cu(II) atoms, one itp ligands, half 1,4-bdc, two halves of coordination hydroxyl (OH⁻), disordered nitrate. The Cu1 atom is coordinated by two OH oxygen atoms (O1/O2), and two nitrogen atoms from two itp ligands in the equatorial positions (N1/N4B) and one Cl⁻ in the apical position in the distorted square-pyramidal configuration (Fig. S1 in the ESI[†]). The structural distortion index τ for Cu1 atom is 0.017, indicating that the coordination environment of the metal atom is closer to square-pyramidal geometry than trigonal-bipyramidal configuration.²¹ The Cu2 atom is coordinated by one OH oxygen atoms (O1), one carboxylate oxygen atom from one 1,4-bdc ligands (O5C) and two nitrogen atoms from two itp ligands (N2/N2A) in the equatorial positions and one carboxylate

oxygen atom from one 1,4-bdc ligand in the apical position (O3) in the distorted square-pyramidal configuration. The structural distortion index τ for Cu2 atom is 0.172, indicating that the coordination environment of the metal atom is closer to square-pyramidal geometry than trigonal-bipyramidal configuration.²¹

The μ₃-OH hydroxy (O1) acts as 3-connected bridge and connects three Cu(II) atoms (Cu1, Cu1A, Cu2) (Fig. 1a). The μ₂-OH hydroxy (O2) acts as 2-connected bridge and connects two Cu(II) atoms (Cu1, Cu1A). Three Cu(II) atoms (Cu1, Cu1A, Cu2) are linked together by one μ₃-OH (O1) and one μ₂-OH (O2), and form [Cu₃(μ₃-OH)(μ₂-OH)] trimeric cluster. Each Cl⁻ acts as bridge and connects three [Cu₃(μ₃-OH)(μ₂-OH)] trimeric cluster trimeric clusters. Three [Cu₃(μ₃-OH)(μ₂-OH)] trimeric cluster trimeric clusters are joined by double μ₃-Cl and construct [Cu₉(μ₃-OH)₃(μ₂-OH)₃(μ₃-Cl)₂] nonanuclear copper(II) cluster (Fig. 1a).

Although few nonanuclear copper(II) clusters were reported.²² For example, $\{[Cu_9(oxamate)_2][Cu(itp)_6](ClO_4)_6 \cdot 12H_2O\}_n$ (oxamate = N,N',N''-1,3,5-benzenetris, pmdien = N,N,N',N'',N''-pentamethyldiethylenetriamine) exhibits the anticipated pattern of six external [Cu(pmdien)]²⁺ subunits ligated to a central [Cu₉(oxamate)₂]⁶⁻ unit.^{22a} [Cu₉(cpida)₆(MeOH)₆]-6(MeOH)

(H₃c-pida = 2-(carboxyphenyl)iminodiacetic acid) is made up of two carboxylate-bridged Cu^{II} units that are linked through a central Cu^{II} to give a Cu₉ core.^{22b} [Cu₉(L)₄(μ₃-OH)₄(MeOH)₂](ClO₄)₂ (H₃L = N,N'-(2-hydroxypropane-1,3-diyl)bis(benzoylacetonimine)) consists of four dinuclear [Cu₂L]⁺ units linked covalently to a central copper atom by four μ₃-OH, thus yielding the nonacopper core.^{22c} [Cu₉(L)₆](BF₄)₆·3CH₃CN·1-PrOH·13H₂O and [Cu₂Cu₇(L)₆](PF₆)₄·4CH₃CN·2CH₃OH·2H₂O (L = 2,6-bis[5-(2-pyridinyl)-1H-pyrazol-3-yl]pyridin) show [3 × 3] copper grid structures.^{22d} [Cu₉(μ₃-OH)₄(μ₂-OH)₂] cluster in {(Cu₉(OH)₆(bte)₂(sip)₄(H₂O)₃·6H₂O} (bte = 1,2-bis(1,2,4-triazol-1-yl)ethane, sip = 5-sulfoisophthalate) can be described as consisting of two [Cu₄(μ₃-OH)₂] moieties connected to a centrally placed Cu(II) ion through two μ₂-OH groups.^{22e} In the cation [Cu₉(L)₃(OH)₇]⁵⁺ of [Cu₉(L)₃(OH)₇](ClO₄)₅·0.25CH₃OH·1.15H₂O (H₂L = 2,2'-((5-methyl-1,3-phenylene)bis(methylene)bis((pyridine-2-ylmethyl)azane-diyl)bis(methyl)bis(4-methylphenol))), a tricopper core is an incomplete cubane with one missing, constructed by three hexacoordinated copper atoms and four μ₃-OH group and then is surrounded by two layers.^{22f} [(MeSiO_{1.5})₁₈(CuO)₉] is the first observation of nonanuclear metallasilsesquioxane ever.^{22g} However, in **1**, three [Cu₃(μ₃-OH)(μ₂-OH)] trimeric cluster trimeric clusters are joined by double μ₃-Cl and construct [Cu₉(μ₃-OH)₃(μ₂-OH)₃(μ₃-Cl)₂] nonanuclear copper(II) cluster. Such nonanuclear copper(II) cluster [Cu₉(μ₃-OH)₃(μ₂-OH)₃(μ₃-Cl)₂] is not reported until now, as to our best knowledge.

Each itp ligand coordinates three Cu(II) atoms via its two triazole nitrogen atoms (N1/N2) and one imidazole nitrogen atom (N4) (Fig. S2 in the ESI†). The Cu(II) atoms in [Cu₉(OH)₆Cl₂] nonanuclear copper(II) cluster are linked by six itp ligands and stabilize the [Cu₉(μ₃-OH)₃(μ₂-OH)₃(μ₃-Cl)₂] cluster, and form [Cu₉(μ₃-OH)₃(μ₂-OH)₃(μ₃-Cl)₂(itp)₆] cluster (Fig. 1b).

Two carboxylate groups of one 1,4-bdc ligands (O3O4, O5O6) show monodentate mode. Each 1,4-bdc ligand acts as 2-connected bridge (Fig. S3 in the ESI†). Each [Cu₉(μ₃-OH)₃(μ₂-OH)₃(μ₃-Cl)₂(itp)₆] nonanuclear copper(II) cluster connects six [Cu₉(μ₃-OH)₃(μ₂-OH)₃(μ₃-Cl)₂(itp)₆] nonanuclear copper(II) clusters via six 1,4-bdc bridges and construct a 2D cationic network with the cage-like voids (diameter ca. 6.5 Å) (Fig. 1c). The nitrate anions, disordered OH⁻ and water molecules are located in the voids.

To simplify the topology, the nonanuclear copper(II) cluster [Cu₉(μ₃-OH)₃(μ₂-OH)₃(μ₃-Cl)₂(itp)₆] is simplified as one node, and 1,4-bdc ligand is the linker. Thus, the structure of **1-NO₃-OH·20H₂O** is simplified as a 6-connected 2D 3⁶-hxl net.²³ The distances between nodes are 18.438(3) Å (Fig. 1d). Although the 3⁶ tiling or tessellation is common in face- and hexagonal-close packed structures of many elements, it is unusual in coordination polymers or metal-organic frameworks (MOFs) due to the requirement for a six-connecting planar node with a 60° inter-contact angle.²⁴ Only few 3⁶ tessellated 2D net coordination polymers were reported so far.²⁵ The first example of 3⁶ tessellated 2D net coordination polymer should be a Co(II) coordination polymer [CoL₃](ClO₄)₂ (L = 1,4-bis(benzimidazole-1-ylmethyl)-2,3,5,6-tetramethylbenzene) reported by Su and co-workers.^{25a} Yang and co-workers synthesized a hexanuclear heterometal cluster coordination polymer showing 3⁶ 2D net.^{25b} 3⁶ tessellated 2D net coordination polymers contain the metal atoms in the unit do not exceed six, to the best of our knowledge.^{24,25} **1-NO₃-OH·20H₂O** is also the first 2D 3⁶-hxl net based nonanuclear cluster.

Anion Exchange Studies with Cr₂O₇²⁻

The measured and simulated PXRDs confirm the purity of **1-NO₃-OH·20H₂O**. The PXRD pattern of **1-NO₃-OH** (the quest free phase)

was almost identical to that of **1-NO₃-OH·20H₂O** which exhibits that **1-NO₃-OH** maintains the framework (Fig. S4 in the ESI†). **1-NO₃-OH** is a porous cationic framework. The NO₃⁻ and OH⁻ anions are located in the voids of the framework. The anion exchange properties of **1-NO₃-OH** were investigated. The crystals of **1-NO₃-OH** were immersed in an aqueous solution of double molar amount of 2.5 × 10⁻³ mol/L Cr₂O₇²⁻ (equal charge of NO₃⁻ and OH⁻, and Cr₂O₇²⁻). The exchange process was monitored by UV/Vis spectroscopy at intervals based on the intensity variation of the maximum adsorption peak of in solution (257 nm). The concentration of Cr₂O₇²⁻ in solution decreased by 46.9%, 56.1%, 64.2%, 71.6% and 83.4% after 1h, 2h, 4h, 6h and 12h, respectively (Fig. 2), corresponding to capture capacities of 0.938, 1.122, 1.284, 1.432 and 1.668 mol mol⁻¹, respectively. Then the concentration of Cr₂O₇²⁻ was slowly decreased, and the concentration of Cr₂O₇²⁻ and solution color were no obvious changes from 24 h to 48 h. The total 88.1% Cr₂O₇²⁻ was captured by **1-NO₃-OH** after 48 h. The overall capacity of **1-NO₃-OH** to capture Cr₂O₇²⁻ is 1.762 mol mol⁻¹ (154.8 mg g⁻¹) after 48 h. As compare, the the theoretic adsorption capacity of **1-NO₃-OH** to capture Cr₂O₇²⁻ is 2.000 mol mol⁻¹ (175.7 mg g⁻¹). The dark teal crystals **1-NO₃-OH** were transfer to green crystals **1-Cr₂O₇²⁻** after **1-NO₃-OH** capturing Cr₂O₇²⁻ anions (Fig. 3).

Adsorption capacities for chromate or dichromate on various porous materials are listed in Table S3 in the ESI† for comparison. For adsorption capacities for dichromate (Cr₂O₇²⁻) on cationic MOF porous materials which were characterized by X-ray diffractometer, the capture capacities of Fir-53, Fir-54,^{13b} a 3D MOF tetranuclear copper(II) cluster (**1-Br**),^{13c} {[Ag(L)₂](BF₄)_n},^{12c} and a 2D Cd based MOF^{12d} were 74.2, 103.1, 128, 81.9 and 116.6 mg/g, respectively. The capture capacity of **1-NO₃-OH** to capture Cr₂O₇²⁻ 154.8 mg g⁻¹ is better than these of above of cationic MOFs, but lower than 166mg/g for a 3D Ni based MOF12b and 207 mg/g for a 3D Ag based MOF.^{13d} A post-synthesized Zr-MOF (**ZJU-101**),^{12a} a Zr-MOF (**MOR-2** via power X-ray crystallography) and its composite MOR-2-HA¹⁴ exhibit the high adsorption capacity for dichromate 245, 193.7 and 162.8 mg/g respectively. For other types adsorbents, the adsorption capacities for Cr(VI) of amino starch, β-CD and quaternary ammonium groups modified cellulose, hexadecylpyridinium bromide modified natural zeolites, modified magnetic chitosan chelating resin and amino-functionalized titanate nanotubes were 12.12, 61.05, 14.31, 58.48 and 153.85 mg/g, respectively.²⁶

When using equimolar amount of **1-NO₃-OH** for absorb dichromate (Cr₂O₇²⁻) under the same conditions, 22.4%, 44.3%, 52.6% and 62.5% of Cr₂O₇²⁻ were exchanged after 5min, 15min, 30min and 60min, respectively (Fig. 4). The UV/Vis adsorption intensity of remained almost constant after 6h, thus indicating completion of the exchange process. During exchange, the solution changed from yellow to colourless. The total 96.2% Cr₂O₇²⁻ was captured by **1-NO₃-OH** after 12 h. The absorb procedure using equimolar amount of **1-NO₃-OH** and dichromate (Cr₂O₇²⁻) is obviously faster than that using **1-NO₃-OH** and double molar amount of dichromate (Cr₂O₇²⁻).

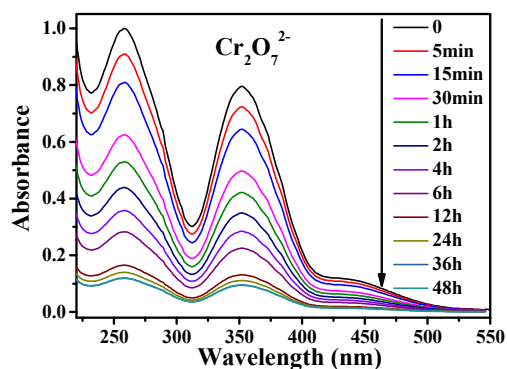


Fig. 2 UV/Vis spectra of $\text{Cr}_2\text{O}_7^{2-}$ aqueous solution during exchange with **1-NO₃-OH** and double molar amount of 2.5×10^{-3} mol/L $\text{Cr}_2\text{O}_7^{2-}$ aqueous solution.

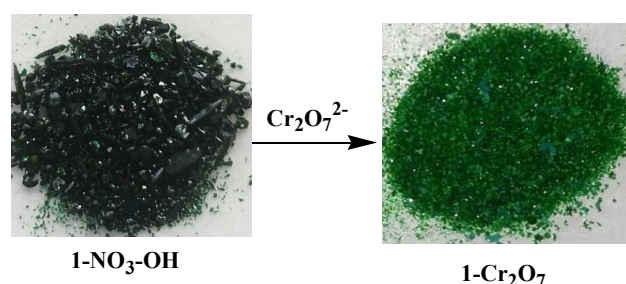


Fig. 3 Colour change of **1-NO₃-OH** crystals to **1-Cr₂O₇** crystals.

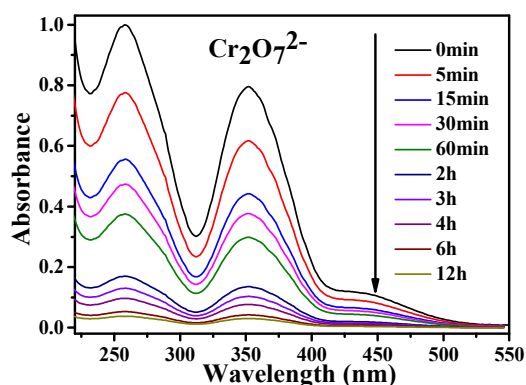


Fig. 4 UV-vis spectra of $\text{Cr}_2\text{O}_7^{2-}$ aqueous solution during anion exchange with equimolar **1-NO₃-OH** and 2.5×10^{-3} mol/L $\text{Cr}_2\text{O}_7^{2-}$ aqueous solution.

The $\text{Cr}_2\text{O}_7^{2-}$ capture ability of **1-NO₃-OH** was further studied in dilute $\text{Cr}_2\text{O}_7^{2-}$ aqueous solution. The crystals of **1-NO₃-OH** were immersed in an equimolar 20ppm $\text{Cr}_2\text{O}_7^{2-}$ aqueous solution. The concentrations of $\text{Cr}_2\text{O}_7^{2-}$ in the solution were decreased by 26.0%, 37.0%, 60.0% and 79.0% after 1h, 2h, 4h and 9h, respectively, as shown in Fig. S4 in the ESI[†]. Then, the concentrations of the $\text{Cr}_2\text{O}_7^{2-}$ were no obvious changes between 36 h and 48 h. The total 87.9% $\text{Cr}_2\text{O}_7^{2-}$ was captured by **1-NO₃-OH** after 48 h.

In comparison with anion exchange, anion selectivity should be more important and challenging. To test the selectivity of the system for $\text{Cr}_2\text{O}_7^{2-}$ capture, selective exchange experiments were

examined for mixtures of anions. When equimolar amount of crystals **1-NO₃-OH** were immersed in the mixed aqueous solution containing 2.5×10^{-3} mol/L $\text{Cr}_2\text{O}_7^{2-}$ and tenfold the molar amount of 2.5×10^{-2} mol/L ClO_4^- , or NO_3^- , Cl^- , BF_4^- or fivefold the molar amount of 1.25×10^{-2} mol/L SO_4^{2-} . The UV/Vis spectroscopy, PXRD (Fig. S5 in the ESI[†]) and FTIR spectroscopy were employed to study the preferential anion uptake. The total $\text{Cr}_2\text{O}_7^{2-}$ captured by **1-NO₃-OH** after 24 h were 63.0%, 78.5%, 80.0%, 81.0% and 85.0% for the mixtures of $\text{Cr}_2\text{O}_7^{2-}/\text{ClO}_4^-$, $\text{Cr}_2\text{O}_7^{2-}/\text{NO}_3^-$, $\text{Cr}_2\text{O}_7^{2-}/\text{Cl}^-$, $\text{Cr}_2\text{O}_7^{2-}/\text{BF}_4^-$ and $\text{Cr}_2\text{O}_7^{2-}/\text{SO}_4^{2-}$, respectively (Fig. 5). The bands corresponding to $\text{Cr}_2\text{O}_7^{2-}$ anion at 940 cm^{-1} were observed in the FTIR spectra of **1-NO₃-OH** after anion exchange (change to **1-Cr₂O₇**) in the presence of interfere anions (Fig. S6 in the ESI[†]). The bands corresponding to the competing anions BF_4^- , Cl^- and SO_4^{2-} were absent. The band corresponding to NO_3^- anion at 1373 cm^{-1} was obviously reduced in the FTIR spectra of **1-NO₃-OH** after anion exchange in the presence of different interfere anions ClO_4^- , NO_3^- , Cl^- , BF_4^- and SO_4^{2-} . The characteristic adsorption band arising from ClO_4^- at about 1084 cm^{-1} was observed. The experiment measurements indicated that the uptake is almost not disturbed by NO_3^- , Cl^- , BF_4^- and SO_4^{2-} . The tenfold the molar amount of ClO_4^- anion has some competitor to $\text{Cr}_2\text{O}_7^{2-}$ anion.

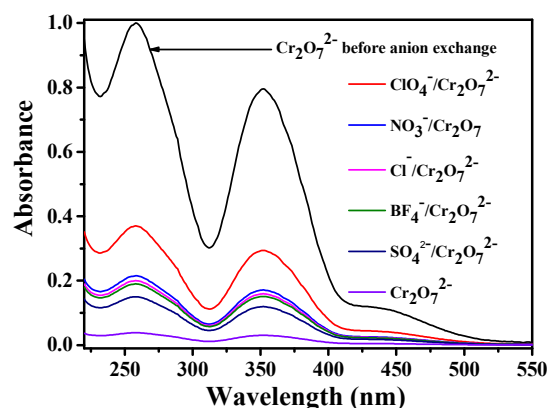


Fig. 5 UV-vis spectra of the mixed aqueous solution during anion exchange.

The trapping and release experiments were carried out to evaluate the regeneration ability of the anion exchange. When 200-fold molar amount of NO_3^- was used as the triggers, 95.7% of $\text{Cr}_2\text{O}_7^{2-}$ was released from **1-Cr₂O₇** after 48 h at first cycle. The trapping and releasing process was performed five continuous cycles. The trapping efficiency was approximate 83.6% at fifth cycle. The release efficiency was approximate 86.8% at fifth cycle.

Anion Exchange Studies with CrO_4^{2-}

The crystals of **1-NO₃-OH** were immersed in an aqueous solution of double molar amount of 2.5×10^{-3} mol/L CrO_4^{2-} (equal charge of NO_3^- and OH^- , and CrO_4^{2-}). The concentrations of CrO_4^{2-} in solution were decreased by 72.2%, 76.9%, 82.7% and 85.6% after 1h, 2h, 4h and 6h, respectively (Fig. 6), corresponding to the capture capacities of 1.444, 1.538, 1.654 and 1.712 mol mol⁻¹, respectively. Then, the concentrations of CrO_4^{2-} were slowly decreased, and the concentrations of CrO_4^{2-} and solution color were no obvious changes from 24 h to 36 h. The total 94.8% CrO_4^{2-} was captured by **1-NO₃-OH** after 36 h. The overall capacity of **1-NO₃-OH** to capture CrO_4^{2-} is 1.896 mol mol⁻¹ (89.5 mg g⁻¹) after 36 h. As compare, the theoretic adsorption capacity of **1-NO₃-OH** to capture CrO_4^{2-} is 2.000 mol mol⁻¹ (94.4 mg g⁻¹). The dark teal crystals **1-NO₃-OH** were

ARTICLE

Journal Name

transfer to bright green crystals **1-CrO₄** after **1-NO₃-OH** capturing CrO_4^{2-} anions (Fig. 7).

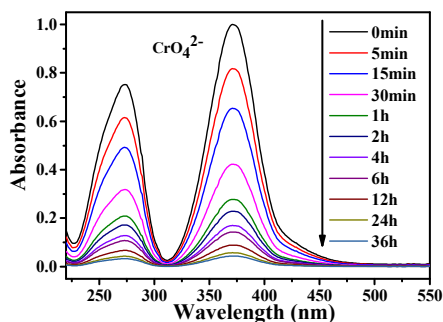


Fig. 6 UV/Vis spectra of CrO_4^{2-} aqueous solution during exchange with **1-NO₃-OH** and double molar amount of 2.5×10^{-3} mol/L CrO_4^{2-} aqueous solution.

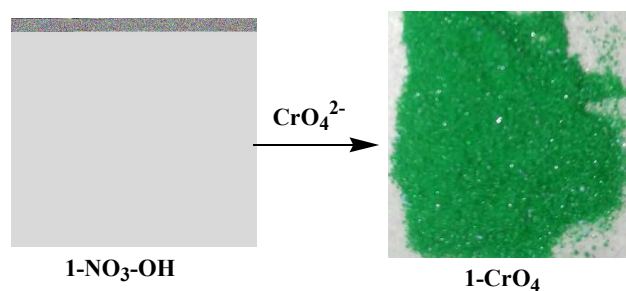


Fig. 7 Colour change of **1-NO₃-OH** crystals to **1-CrO₄** crystals.

The adsorption capacities for capturing CrO_4^{2-} of a 2D Ag based-MOF (**SLUG-21**), a 3D Dy-MOF (**1-ClO₄**) and $\text{Zn}_{0.5}\text{Co}_{0.5}\text{SLUG-35}$ are 60, 62.88 and 68.5 mg g^{-1} , respectively (Table S3 in the ESI[†]).¹¹ The capture capacity 89.5 mg g^{-1} for capturing CrO_4^{2-} of **1-NO₃-OH** is better than these of above cationic MOF. Recently, Lazarides and co-workers reported a Zr MOF (MOR-2) via power X-ray crystallography and its composite form MOR-2-HA which exhibit high adsorption capacities of 118.3 and 109 mg g^{-1} , respectively, for capturing CrO_4^{2-} .¹⁴

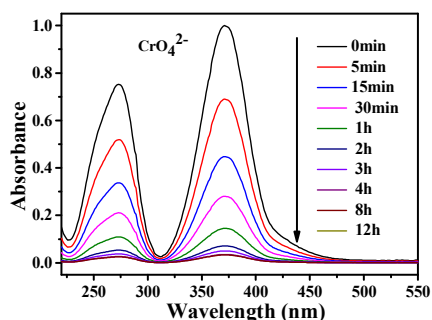


Fig. 8 UV-vis spectra of $\text{Cr}_2\text{O}_7^{2-}$ aqueous solution during anion exchange with equimolar **1-NO₃-OH** and 2.5×10^{-3} mol/L CrO_4^{2-} aqueous solution.

When using equimolar amount of **1-NO₃-OH** for adsorb chromate (CrO_4^{2-}) under the same conditions, 71.9%, 85.5%, 92.9% and 95.0%

of CrO_4^{2-} were exchanged after 30min, 1h, 2h and 4h, respectively (Fig. 8). The UV/Vis adsorption intensity of remained almost constant after 6h, thus indicating completion of the exchange process. During exchange, the solution changed from yellow to colourless. The total 96.7% CrO_4^{2-} was captured by **1-NO₃-OH** after 12 h.

The CrO_4^{2-} capture ability was further investigated in dilute CrO_4^{2-} aqueous solution. The crystals of **1-NO₃-OH** were immersed in an aqueous solution of equimolar 20ppm CrO_4^{2-} . The concentration of CrO_4^{2-} in the solution decreased by 44.0%, 62.4%, 78.2% and 89.7% after 1h, 2h, 4h and 8h, respectively, as shown in Fig. S7 in the ESI[†]. Then, the concentrations of the CrO_4^{2-} were no obvious changes between 12 h and 24 h. The total 91.8% CrO_4^{2-} was captured by **1-NO₃-OH** after 24 h.

When equimolar amount of crystals **1-NO₃-OH** were immersed in the mixed aqueous solution containing 2.5×10^{-3} mol/L CrO_4^{2-} and tenfold the molar amount of 2.5×10^{-2} mol/L ClO_4^- , or NO_3^- , Cl^- , BF_4^- or fivefold the molar amount of 1.25×10^{-2} mol/L SO_4^{2-} . The UV/Vis spectroscopy, PXRD (Fig. S8 in the ESI[†]) and FTIR spectroscopy were employed to study the preferential anion uptake. The total CrO_4^{2-} captured by **1-NO₃-OH** after 24 h were 65.4%, 90.0%, 89.1%, 91.0% and 53.0% for the mixtures of $\text{CrO}_4^{2-}/\text{ClO}_4^-$, $\text{CrO}_4^{2-}/\text{NO}_3^-$, $\text{CrO}_4^{2-}/\text{Cl}^-$, $\text{CrO}_4^{2-}/\text{BF}_4^-$ and $\text{CrO}_4^{2-}/\text{SO}_4^{2-}$, respectively (Fig. S9 in the ESI[†]). The bands corresponding to CrO_4^{2-} anion at about 895 cm^{-1} were observed in the FTIR spectra of **1-NO₃-OH** after anion exchange (change to **1-CrO₄**) in the presence of interfere anions (Fig. S10 in the ESI[†]).^{11c} The bands corresponding to NO_3^- anions at 1373 cm^{-1} were obviously reduced in the FTIR spectra **1-NO₃-OH** after anion exchange (change to **1-CrO₄**) in the presence of different interfere anions ClO_4^- , NO_3^- , Cl^- , BF_4^- and SO_4^{2-} . The bands corresponding to the competing anions BF_4^- and Cl^- were absent in the FTIR spectra. The characteristic adsorption bands arising from ClO_4^- at about 1084 cm^{-1} and SO_4^{2-} at about 1103 cm^{-1} were observed. The measurements indicated that the uptake of is almost not disturbed by NO_3^- , Cl^- and BF_4^- . The tenfold the molar amount of ClO_4^- anion and fivefold the molar amount of SO_4^{2-} anion have some competitor to CrO_4^{2-} anion.

When 200-fold molar amount of NO_3^- was used as the triggers, 96.3% of $\text{Cr}_2\text{O}_7^{2-}$ was released from **1-CrO₄** after 48 h at first cycle. The trapping and releasing process was performed five continuous cycles. The trapping efficiency was approximate 84.3% at fifth cycle. The release efficiency was approximate 88.2% at fifth cycle.

1-NO₃-OH shows the selectivity capture for $\text{Cr}_2\text{O}_7^{2-}$ or CrO_4^{2-} . The anions NO_3^- and OH^- located in the the cage-like voids (diameter ca. 6.5 \AA) of **1-NO₃-OH** were exchanged by $\text{Cr}_2\text{O}_7^{2-}$ or CrO_4^{2-} because the shape and size of relative big $\text{Cr}_2\text{O}_7^{2-}$ and tetrahedral CrO_4^{2-} anions are more suitable for the big cage-like voids than other small competing anions ClO_4^- , NO_3^- , Cl^- , BF_4^- and SO_4^{2-} . Moreover, the probable O-H \cdots O hydrogen bonding interactions between the coordinated hydroxyl groups and $\text{Cr}_2\text{O}_7^{2-}$ or CrO_4^{2-} can support the MOF' selectivity capture for $\text{Cr}_2\text{O}_7^{2-}$ or CrO_4^{2-} .

Catalytic activity for the degradation of methylene blue and rhodamine B

The UV-vis spectrum (Fig. S11 in the ESI[†]) of **1-NO₃-OH**·20H₂O sample shows the absorption peak at 480 nm, which should be caused by the optical transitions of the ligand-to-metal charge transfer (LMCT). The band gap energy (E_g) is estimated to be 2.06 eV by the extraction of the linear portion of the absorption edge, indicating its semiconductor nature.

To study the photocatalytic activity of **1-NO₃-OH-20H₂O**, we selected the cationic organic dyes methylene blue (MB), and rhodamine B (RhB) as the model dye contaminants to evaluate the photocatalytic effectiveness under visible light irradiation in the purification of wastewater.¹⁶⁻¹⁹

The photocatalytic behaviors of **1-NO₃-OH-20H₂O** for the degradation of MB under visible light irradiation were shown in Fig. 9 and Fig. 10. After 90 min, the degradation efficiency of MB reached 92.5% in the presence of catalyst **1-NO₃-OH-20H₂O**. However, the degradation efficiency of MB was reduced to 19.8% after 90 min when the experiment was conducted in the presence of only H₂O₂ and in the absence of catalyst. Therefore, **1-NO₃-OH-20H₂O** is a good catalyst for the degradation of MB.

The photocatalytic behaviors of **1-NO₃-OH-20H₂O** for the degradation of RhB under visible light irradiation were shown in Fig. 11 and Fig. 12. After 120 min, the degradation efficiency of RhB reached 92.1% in the presence of catalyst **1-NO₃-OH-20H₂O**. However, the degradation efficiency of RhB was reduced to 14.0% after 120 min when the experiment was conducted in the presence of only H₂O₂. Therefore, **1-NO₃-OH-20H₂O** is also a good catalyst for the degradation of RhB.

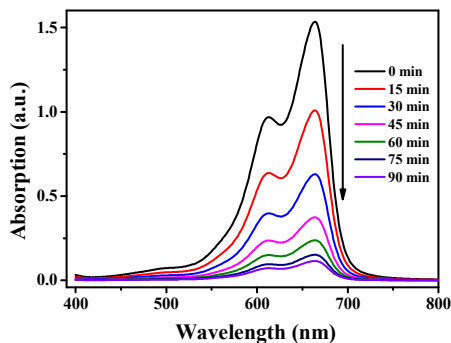


Fig. 9 The UV-vis absorption spectra of MB solution during photocatalytic degradation of the MB solution using catalyst **1** in the presence of H₂O₂ under visible light irradiation.

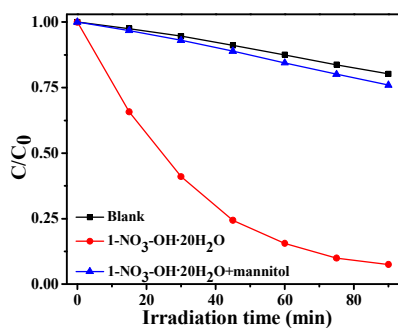


Fig. 10 Photocatalytic degradation efficiencies of the MB solution using catalyst **1-NO₃-OH-20H₂O** in the presence H₂O₂ or H₂O₂ and mannitol, and only H₂O₂ under visible light irradiation.

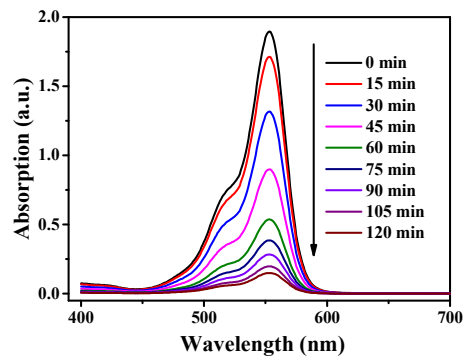


Fig. 11 The UV-vis absorption spectra of RhB solution during photocatalytic degradation of the MB solution using catalyst **1-NO₃-OH-20H₂O** in the presence of H₂O₂ under visible light irradiation.

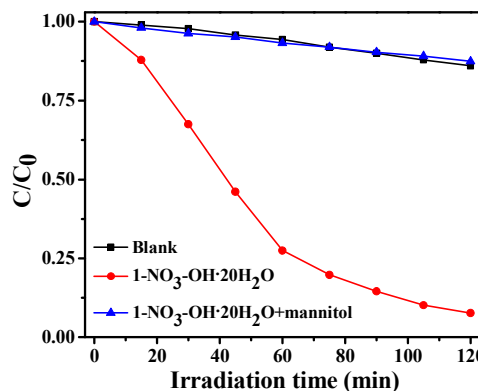


Fig. 12 Photocatalytic degradation efficiencies of the RhB solution using catalyst **1-NO₃-OH-20H₂O** in the presence H₂O₂ or H₂O₂ and mannitol, and only H₂O₂ under visible light irradiation.

After the photocatalytic experiment, the PXRD patterns of **1-NO₃-OH-20H₂O** are in good agreement with that of the original **1-NO₃-OH-20H₂O**, implying that **1-NO₃-OH-20H₂O** after the photocatalytic reaction maintains their structural integrity (Fig. S12 in ESI[†]). The photocatalytic experiment proves that **1-NO₃-OH-20H₂O** is a highly efficient photocatalyst for degradation of the cationic organic dyes MB and RhB.

In order to reveal the photocatalytic mechanism, the photocatalytic reactions were performed under the same conditions using catalyst **1-NO₃-OH-20H₂O** in the presence of mannitol (1.0 g).^{17,18} The experimental results (Fig. 10 and Fig. 12) show that the catalytic activity of **1-NO₃-OH-20H₂O** almost completely disappeared in the presence of mannitol (1.0 g) and reveal that the photogenerated holes should be the active species for the dye degradation process. The oxidation ability of the holes is determined by the energy position of the valence band. The VB XPS spectrum (Fig. S13 in the ESI[†]) shows that the VB edge of **1-NO₃-OH-20H₂O** locates at 0.62 eV.^{17,18f}

The holes also can oxidize hydroxyl ions (OH⁻) to generated the [•]OH radicals. The hydroxyl radicals can directly oxidize the dyes. The

ARTICLE

Journal Name

$\cdot\text{OH}$ radicals can also react with terephthalic acid (TA) in the solution to generate 2-hydroxyterephthalic acid (TAOH), which emits a unique fluorescence signal with its peak at ca. 426 nm.^{17i,18f} The intensity of the TAOH fluorescence signal can qualitatively identify the amount of the generated $\cdot\text{OH}$ radicals. As shown in Fig. S14, samples reacting for 10 min were selected as the objects of photoluminescence spectra. There was a lack of the signal of TAOH without the photocatalyst and H_2O_2 . The TAOH fluorescent peak was observed when H_2O_2 was added. A relative strong fluorescence was detected in the presence of only photocatalyst **1-NO₃-OH-20H₂O**. The remarkably increased TAOH fluorescence intensity in the presence of **1-NO₃-OH-20H₂O** and H_2O_2 confirms that the photocatalyst system in the presence of photocatalyst **1-NO₃-OH-20H₂O** and H_2O_2 can generate more $\cdot\text{OH}$ radicals.

Therefore, the photocatalytic reaction mechanism could be assumed. The photocatalyst **1-NO₃-OH-20H₂O** was irradiated by photons with energy equal to or greater than the band gap (2.06 eV), electrons are excited from the valence band (VB) to the conduction band, leaving the holes in the valence band. The photogenerated holes have a strong oxidant ability and can directly oxidize dyes or can react with hydroxyl ions to generate hydroxyl radicals. The hydroxyl radicals can directly oxidize the dyes to effectively decompose the organic dyes (MB, RhB) to complete the photocatalytic process.

Conclusions

A bifunctional cationic metal-organic framework **1-NO₃-OH-20H₂O** was synthesized and characterized. **1-NO₃-OH-20H₂O** shows a 6-connected 2D 3⁶-hxl net based on unprecedented nonanuclear copper(II) cluster $[\text{Cu}_9(\mu_3\text{-OH})_3(\mu_2\text{-OH})_3(\mu_3\text{-Cl})_2]$. **1-NO₃-OH-20H₂O** is also the first 2D 3⁶-hxl net based nonanuclear cluster. **1-NO₃-OH** (guest-free phase) shows fast and high efficient $\text{Cr}_2\text{O}_7^{2-}$ and CrO_4^{2-} trapping, and good recyclability for capturing of $\text{Cr}_2\text{O}_7^{2-}$ and CrO_4^{2-} . **1-NO₃-OH-20H₂O** exhibits highly efficient photocatalytic degradation of the cationic organic dyes methylene blue (MB) and rhodamine B (RhB) under visible light irradiation.

In summary, a stable cationic MOF was synthesized. The present results could provide a good cationic MOF sorbent for removal of hexavalent chromium pollutants and a good photocatalyst for removal of organic dye pollutants in wastewater.

Conflicts of interest

There are no conflicts to declare.

Acknowledgements

This work is supported by the National Natural Science Foundation of China (No. 21171126), the Natural Science Foundation of Jiangsu Province (No. BK20161212), the Priority Academic Program Development of Jiangsu Higher Education Institutions, State and Local Joint Engineering Laboratory for Functional Polymeric Materials, and the project of scientific and technological infrastructure of SuZhou (SZS201708).

Notes and references

- 1 F. Fu and Q. Wang, *J. Environ. Manage.*, 2011, **92**, 407.
- 2 L. H. Keith and W. A. Teillard, *Environ. Sci. Technol.*, 1979, **13**, 416.
- 3 (a) M. Costa and C. B. Klein, *Crit. Rev. Toxicol.*, 2006, **36**, 155; (b) L. Khezami and R. Capart, *J. Hazard. Mater.*, 2005, **123**, 223; (c) A. Zhitkovich, *Chem. Res. Toxicol.*, 2005, **18**, 3.
- 4 (a) L. Li, L. Fan, M. Sun, H. Qiu, X. Li, H. Duan and C. Luo, *Colloids Surf., B*, 2013, **107**, 76; (b) S. V. Prasanna and P. Vishnu Kamath, *Solid State Sci.*, 2008, **10**, 260; (c) C. V. Gherasim and G. Bourceanu, *Chem. Eng. J.*, 2013, **220**, 24.
- 5 W. W. Li, H. Q. Yu and Z. He, *Energy Environ. Sci.*, 2013, **7**, 911.
- 6 (a) T. Aarthi and G. Madras, *Catal. Commun.*, 2008, **9**, 630; (b) T. Jing, Y. Dai, W. Wei, X. C. Ma and B. B. Huang, *Phys. Chem. Phys.*, 2014, **16**, 18596; (c) J. Di, J. Xia, Y. Ge, H. Li, H. Ji, H. Xu, Q. Zhang, H. Li and M. Li, *Appl. Catal. B*, 2015, **168**, 51; (d) H. Wang, M. Miyauchi, Y. Ishikawa, A. Pyatenko, N. Koshizaki, Y. Li, L. Li, X. Li, Y. Bando and D. Golberg, *J. Am. Chem. Soc.*, 2011, **133**, 19102; (e) Z. Sha, J. Sun, H.S.O. Chan, S. Jaenicke and J. Wu, *RSC Adv.*, 2014, **4**, 64977.
- 7 (a) M. N. Chong, B. Jin and C. W. K. Chow, *Water Res.*, 2010, **44**, 2997; (b) E. Piera, M. I. Tejedor-Tejedor, M. E. Zorn and M. A. Anderson, *Appl. Catal. B*, 2003, **46**, 671.
- 8 (a) S. M. Cohen, *Chem. Rev.*, 2012, **112**, 970; (b) H. Li, M. Eddaoudi, M. O'Keeffe and O. M. Yaghi, *Nature*, 1999, **402**, 276; (c) R. Matsuda, R. Kitaura, S. Kitagawa, Y. Kubota, R. V. Belosludov, T. C. Kobayashi, H. Sakamoto, T. Chiba, M. Takata, Y. Kawazoe and Y. Mita, *Nature*, 2005, **436**, 238; (d) J. R. Long, O. M. Yaghi, *Chem. Soc. Rev.*, 2009, **38**, 1213; (e) G. Ferey and C. Serre, *Chem. Soc. Rev.*, 2009, **38**, 1380; (f) E. Coronado and G. M. Espallargas, *Chem. Soc. Rev.*, 2013, **42**, 1525; (g) I. Stassen, N. Burtch, A. Talin, P. Falcaro, M. Allendorf and R. Ameloot, *Chem. Soc. Rev.*, 2017, **46**, 3185; (h) M. M. Sadiq, H. Li, A. J. Hill, P. Falcaro, M. R. Hill, K. Suzuki, *Chem. Mater.*, 2016, **28**, 6219; (i) L. E. Kreno, O. K. Farha, M. Allendorf, R. P. Van Duyne and J. T. Hupp, *Chem. Rev.*, 2012, **112**, 1105.
- 9 (a) M. Mon, J. Ferrando-Soria, T. Grancha, F.R. Fortea-Pérez, J. Gascon, A. Leyva-Pérez, D. Armentano and E. Pardo, *J. Am. Chem. Soc.*, 2016, **138**, 7864; (b) F. Vermoortele, M. Vandichel, B. V. de Voorde, R. Ameloot, M. Waroquier, V. V. Speybroeck and D. E. De Vos, *Angew. Chem. Int. Ed.*, 2012, **51**, 4887; (c) Y. Y. Hu, T. T. Zhang, X. Zhang, D. C. Zhao, X. B. Cui, Q. S. Huo and J. Q. Xua, *Dalton Trans.*, 2016, **45**, 2562; (d) S. T. Zheng, T. Wu, C. Chou, A. Fuhr, P. Y. Feng and X. H. Bu, *J. Am. Chem. Soc.*, 2012, **134**, 4517; (e) X. X. Liu, C. D. Shi, C. W. Zhai, M. L. Cheng, Q. Liu, G. X. Wang, *ACS Appl. Mater. Interfaces*, 2016, **8**, 4585; (f) M. X. Li, Y. F. Zhang, X. He, X. M. Shi, Y. P. Wang, M. Shao and Z. X. Wang, *Cryst. Growth Des.*, 2016, **16**, 2912; (g) X. G. Liu, H. Wang, B. Chen, Y. Zou, Z. G. Gu, Z. J. Zhao and L. Shen, *Chem. Commun.*, 2015, **51**, 1677; (h) S. S. Zhang, X. Wang, H. F. Su, L. Feng, Z. Wang, W. Q. Ding, V. A. Blatov, M. Kurmoo, C. H. Tung, D. Sun and L. S. Zheng, *Inorg. Chem.*, 2017, **56**, 11891; (i) Z. J. Lin, H. Q. Zheng, H. Y. Zheng, L. P. Lin, Q. Xin and R. Cao, *Inorg. Chem.*, 2017, **56**, 14178.
- 10 (a) D. T. Tran, P. Y. Zavalij and S. R. J. Oliver, *J. Am. Chem. Soc.*, 2002, **124**, 3966; (b) M. Du, X. J. Zhao, J. H. Guo and S. R. Batten, *Chem. Commun.*, 2005, 4836; (c) T. K. Maji, R. Matsuda and S. Kitagawa, *Nat. Mater.*, 2007, **6**, 142; (d) C. Fang, Q. K. Liu, J. P. Ma and Y. B. Dong, *Inorg. Chem.*, 2012, **51**, 3923; (e) B. Manna, A. K. Chaudhari, B. Joarder, A. Karmakar and S. K. Ghosh, *Angew. Chem. Int. Ed.*, 2013, **52**, 998; (f) B. H. Hamilton, T. A. Wagler, M. P. Espe and C. J. Ziegler, *Inorg. Chem.*, 2005, **44**, 4891; (g) H. Fei and S. R. J. Oliver, *Angew. Chem. Int. Ed.*, 2011, **50**, 9066; (h) H. H. Fei, D. L. Rogow and S. R. J. Oliver, *J. Am. Chem. Soc.*, 2010, **132**, 7202; (i) (b) R. Cao, B. D. McCarthy and S. J. Lippard, *Inorg. Chem.*, 2011, **50**, 9499; (j) R. Custelcean, P. V. Bonnesen, N.

- C. Duncan, X. Zhang, L. A. Watson, G. V. Berkel, W. B. Parson and B. P. Hay, *J. Am. Chem. Soc.*, 2012, **134**, 8525; (k) S. Wang, P. Yu, B. A. Purse, M. J. Orta, J. Diwu, W. H. Casey, B. L. Phillips, E. V. Alekseev, W. Depmeier, D. T. Hobbs and T. E. Albrecht-Schmitt, *Adv. Funct. Mater.*, 2012, **22**, 2241.
- 11 (a) H. Fei, M. R. Bresler and S. R. J. Oliver, *J. Am. Chem. Soc.*, 2011, **133**, 11110; (b) P. F. Shi, B. Zhao, G. Xiong, Y. L. Hou and P. Cheng, *Chem. Commun.*, 2012, **48**, 8231; (c) H. Fei, C. S. Hen, J. C. Robins and S. R. J. Oliver, *Chem. Mater.*, 2013, **25**, 647.
- 12 (a) Q. Zhang, J. Yu, J. Cai, L. Zhang, Y. Cui, Y. Yang, B. Chen and G. Qian, *Chem. Commun.*, 2015, **51**, 14732; (b) A. V. Desai, B. Manna, A. Karmakar, A. Sahu and S. K. Ghosh, *Angew. Chem., Int. Ed.*, 2016, **55**, 7811; (c) K. Nath, K. Maity and K. Biragha, *Cryst. Growth Des.*, 2017, **17**, 4437; (d) H. R. Fu, Y. Zhao, Z. Zhou, X. G. Yang and L. F. Ma, *Dalton Trans.*, 2018, **47**, 3725.
- 13 (a) X. Li, H. Xu, F. Kong and R. Wang, *Angew. Chem., Int. Ed.*, 2013, **52**, 13769; (b) H. R. Fu, Z. X. Xu and J. Zhang, *Chem. Mater.*, 2015, **27**, 205; (c) X. X. Lv, L. L. Shi, K. Li, B. L. Li and H. Y. Li, *Chem. Commun.*, 2017, **53**, 1860; (d) C. P. Li, H. Zhou, S. Wang, J. Chen, Z. L. Wang and M. Du, *Chem. Commun.*, 2017, **53**, 9206.
- 14 S. Rapti, D. Sarma, S. A. Diamantis, E. Skliri, G. S. Armatas, A. C. Tsipis, Y. S. Hassan, M. Alkordi, C. D. Malliakas, M. G. Kanatzidis, T. Lazarides and J. C. Plakatouras, *J. Mater. Chem. A*, 2017, **5**, 14707.
- 15 M. Alvaro, E. Carbonell, B. Ferrer, F.X.L. Xamena and H. Garcia, *Chem. Eur. J.*, 2007, **13**, 5106.
- 16 (a) Y. Hu, F. Luo, F. F. Dong, *Chem. Commun.*, 2011, **47**, 761; (b) G. H. Cui, C. H. He, C. H. Jiao, J. C. Geng and V. A. Blatov, *CrystEngComm*, 2012, **14**, 4210; (c) L. Liu, J. Ding, M. Li, X. Lv, J. Wu, H. Hou and Y. Fan, *Dalton Trans.*, 2014, **43**, 12790; (d) J. W. Cui, S. X. Hou, K. V. Heckeb and G. H. Cui, *Dalton Trans.*, 2017, **46**, 2892; (e) J. J. Du, Y. P. Yuan, J. X. Sun, F. M. Peng, X. Jiang, L. G. Qiu, A. J. Xie, Y. H. Shen and J. F. Zhu, *J. Hazard. Mater.*, 2011, **190**, 945.
- 17 (a) H. X. Yang, T. F. Liu, M. N. Cao, H. F. Li, S. Y. Gao and R. Cao, *Chem. Commun.*, 2010, **46**, 2429; (b) T. Wen, D. X. Zhang, J. Liu, R. Lin and J. Zhang, *Chem. Commun.*, 2013, **49**, 5660; (c) B. Q. Song, X. L. Wang, C. Y. Sun, Y. T. Zhang, X. S. Wu, L. Yang, K. Z. Shao, L. Zhao and Z. M. Su, *Dalton Trans.*, 2015, **44**, 13818; (d) P. Y. Wu, Y. H. Liu, Y. Li, M. Jiang, X. L. Li, Y. H. Shi and J. Wang, *J. Mater. Chem. A*, 2016, **4**, 16349; (e) C. K. Wang, F. F. Xing, Y. L. Bai, Y. M. Zhao, M. X. Li and S. R. Zhu, *Cryst. Growth Des.*, 2016, **16**, 2277; (f) N. Hussain, V. K. Bhardwaj, *Dalton Trans.*, 2016, **45**, 7697; (g) Q. Li, D. X. Xue, Y. F. Zhang, Z. H. Zhang, Z. W. Gao and J. F. Bai, *J. Mater. Chem. A*, 2017, **5**, 14182; (h) W. T. Xu, L. Ma, F. Ke, F. M. Peng, G. S. Xu, Y. H. Shen, J. F. Zhu, L. G. Qiu and Y. P. Yuan, *Dalton Trans.*, 2014, **43**, 3792.
- 18 (a) B. Q. Song, X. L. Wang, J. Liang, Y. T. Zhang, K. Z. Shao and Z. M. Su, *CrystEngComm*, 2014, **16**, 9163; (b) L. L. Liu, C. X. Yu, J. M. Du, S. M. Liu, J. S. Cao and L. F. Ma, *Dalton Trans.*, 2016, **45**, 12352; (c) X. L. Wang, X. M. Wu, G. C. Liu, H. Y. Lin and X. Wang, *Dalton Trans.*, 2016, **45**, 19341; (d) Jun Zhao, W. W. Dong, Y. P. Wu, Y. N. Wang, C. Wang, D. S. Li and Q. C. Zhang, *J. Mater. Chem. A*, 2015, **3**, 6962; (e) S. Ou, J. P. Zheng, G. Q. Kong and C. D. Wu, *Dalton Trans.*, 2015, **44**, 7862; (f) J. Y. Li, X. Jiang, L. Lin, J. J. Zhou, G. S. Xu and Y. P. Yuan, *J. Mol. Catal. A-Chem.*, 2015, **406**, 46.
- 19 (a) Y. F. Peng, S. Zhao, K. Li, L. Liu, B. L. Li and B. Wu, *CrystEngComm*, 2015, **17**, 2544; (b) L. Liu, Y. F. Peng, X. X. Lv, Ke Li, B. L. Li and B. Wu, *CrystEngComm*, 2016, **18**, 2490; (c) L. L. Shi, T. R. Zheng, M. Li, L. L. Qian, B. L. Li, H. Y. Li, *RSC Adv.*, 2017, **7**, 23432.
- 20 (a) G. M. Sheldrick, *Acta Cryst. A*, 2008, **64**, 112; (b) G. M. Sheldrick, *Acta Cryst. C*, 2015, **71**, 3; (c) O. V. Dolomanov, L. J. Bourhis, R. J. Gildea, J. A. K. Howard and H. Puschmann, *J. Appl. Cryst.*, 2009, **42**, 339.
- 21 (a) A. W. Addison, T. N. Rao, J. Reedijk, J. Van Rijn and G. C. Verschoor, *J. Chem. Soc., Dalton Trans.*, 1984, **7**, 1349; (b) B. L. Li, Z. Xu, Z. B. Cao, L. M. Zhu and K. B. Yu, *Trans. Met. Chem.*, 1999, **24**, 622.
- 22 (a) X. Ottenwaelde, J. Cano, Y. Journaux, E. Riviere, C. Brennan, M. Nierlich, R. Ruiz-Garcia, *Angew. Chem., Int. Ed.*, 2004, **43**, 580; (b) M. Murugesu, P. King, P. Clerac, C. E. Anson, A. K. Powell, *Chem. Commun.*, 2004, **740**; (c) S. Khanra, T. Weyhermuller and P. Chaudhuri, *Dalton Trans.*, 2009, 3847; (d) H. Sato, L. Miya, K. Mitsumoto, T. Matsumoto, T. Shiga, G. N. Newton and H. Oshio, *Inorg. Chem.*, 2013, **52**, 9714; (e) X. Zhu, S. Zhao, Y. F. Peng, B. L. Li and B. Wu, *CrystEngComm*, 2013, **15**, 9154; (f) X. L. You, Z. H. Wei, H. L. Wang, D. P. Li, J. Liu, B. B. Xu and X. M. Liu, *RSC Adv.*, 2014, **4**, 61790; (g) A. N. Bilyachenko, A. N. Kulakova, M. M. Levitsky, A. A. Petrov, A. A. Korlyukov, L. S. Shulpina, V. N. Khrustalev, P. V. Dorovatovskii, A. V. Vologzhanina, U. S. Tsareva, I. E. Golub, E. S. Gulyaeva, E. S. Shubina and G. B. Shulpin, *Inorg. Chem.*, 2017, **56**, 4093.
- 23 (a) V. A. Blatov, M. O'Keeffe and D. M. Proserpio, *CrystEngComm*, 2010, **12**, 44; (b) E. V. Alexandrov, V. A. Blatov, A. V. Kochetkov and D. M. Proserpio, *CrystEngComm*, 2011, **13**, 3947; (c) V. A. Blatov, A. P. Shevchenko and V. N. Serezhkin, *J. Appl. Crystallogr.*, 2000, **33**, 1193; (d) V. A. Blatov, A. P. Shevchenko and D. M. Proserpio, *Cryst. Growth Des.*, 2014, **14**, 3576.
- 24 R. J. Hill, D. L. Long, N. R. Champness, P. Hubberstey and M. Schröder, *Acc. Chem. Res.*, 2005, **38**, 337.
- 25 (a) C. Y. Su, Y. P. Cai, C. L. Chen and B. S. Kang, *Inorg. Chem.*, 2001, **40**, 2210; (b) W. H. Fang and G. Y. Yang, *CrystEngComm*, 2014, **16**, 6790; (c) C. A. Williams, A. J. Blake, P. Hubberstey, M. Schröder, *Chem. Commun.*, 2005, 5435; (d) M. Du, X. J. Jiang, X. J. Zhao, *Inorg. Chem.*, 2007, **46**, 3984; (e) H. Y. Chen, D. R. Xiao, J. H. He, Z. F. Li, G. J. Zhang, D. Z. Sun, R. Yuan, E. B. Wang and Q. L. Luo, *CrystEngComm*, 2011, **13**, 4988; (f) J. H. Jia, A. J. Blake, N. R. Champness, P. Hubberstey, C. Wilson and M. Schröder, *Inorg. Chem.*, 2008, **47**, 8652; (g) Z. R. Pan, J. Xu, H. G. Zheng, K. X. Huang, Y. Z. Li, Z. J. Guo and S. R. Batten, *Inorg. Chem.*, 2009, **48**, 5772; (h) L. L. Zhang, F. L. Liu, Y. Guo, X. P. Wang, J. Guo, Y. H. Wei, Z. Chen and D. F. Sun, *Cryst. Growth Des.*, 2012, **12**, 6215; (i) V. Sharma, D. De, S. Pal, P. Saha and P. K. Bharadwaj, *Inorg. Chem.*, 2017, **56**, 8847.
- 26 (a) A. Dong, J. Xie, W. Wang, L. Yu, Q. Liu and Y. Yin, *J. Hazard. Mater.*, 2010, **181**, 448; (b) Y. Zhou, Q. Jin, T. Zhu and Y. Akama, *J. Hazard. Mater.*, 2011, **187**, 303; (c) Y. Zeng, H. Woo, G. Lee and J. Park, *Microporous Mesoporous Mater.*, 2010, **130**, 83; (d) Y. G. Abou El-Reash, M. Otto, I. M. Kenawy and A. M. Ouf, *Int. J. Biol. Macromol.*, 2011, **49**, 513; (e) L. Wang, W. Liu, T. Wang and J. Ni, *Chem. Eng. J.*, 2013, **225**, 153.

A Table of Contents

A bifunctional cationic metal-organic framework shows a 6-connected 2D 3^6 -hxl net based on unprecedented nonanuclear copper(II) cluster, fast and high efficient $\text{Cr}_2\text{O}_7^{2-}$ and CrO_4^{2-} trapping, and highly efficient photocatalytic degradation of the cationic organic dyes methylene blue and rhodamine B under visible light irradiation, under visible light irradiation.

